water

MDPI

Article

Implementation of $FeSO_4 \cdot H_2O$ as an Eco-Friendly Coagulant for the Elimination of Organic Pollutants from Tertiary Palm Oil Mill Effluent: Process Optimization, Kinetics, and Thermodynamics Studies

Md. Sohrab Hossain [1,*], Shabib Al Rashdi [2], Yaman Hamed [3], Adel Al-Gheethi [4], Fatehah Mohd Omar [5], Muzafar Zulkifli [6] and Ahmad Naim Ahmad Yahaya [6,*]

1 HICoE-Centre for Biofuel and Biochemical Research, Institute of Self-Sustainable Building, Department of Fundamental and Applied Sciences, Universiti Teknologi PETRONAS, Seri Iskandar 32610, Perak Darul Ridzuan, Malaysia
2 Waste to Energy Lab, Department of Mechanical and Industrial Engineering, College of Engineering, National University of Science and Technology, Al Hail Caledonian Campus, CPO Seeb 111, Muscat P.O. Box 2322, Oman
3 Centre for Mathematical and Statistical Science, Institution of Autonomous Systems, Department of Fundamental and Applied Sciences, Universiti Teknologi PETRONAS, Seri Iskandar 32610, Perak Darul Ridzuan, Malaysia
4 Micro-Pollutant Research Centre (MPRC), Department of Civil Engineering, Faculty of Civil Engineering and Built and Environment, Universiti Tun Hussein Onn Malaysia, Batu Pahat 83000, Malaysia
5 School of Civil Engineering, Universiti Sains Malaysia, Nibong Tebal 14300, Penang, Malaysia
6 Universiti Kuala Lumpur-Malaysian Institute Chemical and Bioengineering Technology (UniKL-MICET), Alor Gajah 78000, Melaka, Malaysia
* Correspondence: sohrab.hossain@utp.edu.my (M.S.H.); ahmadnaim@unikl.edu.my (A.N.A.Y.)

Abstract: The biologically treated palm oil mill effluent (POME) urges further treatment to minimize the residual pollutant concentration for safe discharge in the nearest watercourse. In the present study, the post-treatment of biologically treated POME was conducted using ferrous sulfate monohydrate ($FeSO_4 \cdot H_2O$) as a coagulant. The influence of the $FeSO_4 \cdot H_2O$ coagulation of POME was determined on the elimination of biochemical oxygen demand (BOD), suspended solids (SS), and chemical oxygen demand (COD) with varying flocculation time (min), slow mixing speed (rpm), coagulant doses (g/L) and pH. The $FeSO_4 \cdot H_2O$ coagulation–flocculation experimental conditions were designed following the central composite design (CCD) of experiments and optimized by employing response surface methodology (RSM) based on the optimal SS, COD, and BOD elimination from POME. The maximum BOD, SS, and COD elimination achieved were about 96%, 97%, and 98%, respectively, at the optimized experimental condition. The surface morphology and elemental composition analyses of raw $FeSO_4 \cdot H_2O$ and sludge generated after coagulation revealed that the $FeSO_4 \cdot H_2O$ effectively removed the colloidal and suspended particles from POME. The well-fitted kinetic model equation was the pseudo-second-order kinetic equation to describe the $FeSO_4 \cdot H_2O$ coagulation–flocculation behavior. The thermodynamics properties analyses revealed that the $FeSO_4 \cdot H_2O$ coagulation of POME was non-spontaneous and endothermic. The residual SS, COD, and BOD in treated POME were determined to be 28.27 ± 5 mg/L, 147 ± 3 mg/L, and 6.36 ± 0.5 mg/L, respectively, lower the recommended discharged limits as reported by the Department of Environment (DoE), Malaysia.

Keywords: coagulation–flocculation; $FeSO_4 \cdot H_2O$; palm oil mill effluent; response surface methodology; sustainability; post-treatment

check for updates

Citation: Hossain, M.S.; Rashdi, S.A.; Hamed, Y.; Al-Gheethi, A.; Omar, F.M.; Zulkifli, M.; Ahmad Yahaya, A.N. Implementation of $FeSO_4 \cdot H_2O$ as an Eco-Friendly Coagulant for the Elimination of Organic Pollutants from Tertiary Palm Oil Mill Effluent: Process Optimization, Kinetics, and Thermodynamics Studies. *Water* **2022**, *14*, 3602. https://doi.org/10.3390/w14223602

Academic Editor: Margaritis Kostoglou

Received: 3 October 2022
Accepted: 2 November 2022
Published: 8 November 2022

1. Introduction

There is an increasing concern about discharging POME into the aquatic environment on account of posing severe environmental pollution. POME is a thick brownish liquid,

engendered through the sterilization of oil palm fruits bunch (OPFB) in a palm oil mill [1,2]. Generally, it requires over six tons of fresh water to produce one ton of palm oil [1,3]. Studies reported that about 3 tons of POME are generated for the processing per ton of palm oil [3,4]. Although POME is a non-toxic industrial effluent, it is considered hazardous industrial effluent for the environment because of contains high SS, COD, and BOD [2,3]. In addition, POME is acidic and odorous; therefore, releasing untreated POME into a waterway may have detrimental effects on aquatic life [2,4]. The environmental agencies in palm oil-producing nations have enforced regulations to safely discharge POME into a water course [5,6]. For instance, the DoE, Malaysia has established industrial effluent discharge limits under the Environment Quality Regulations 1977 [6]. The regulation aims to diminish the residual pollutant concentration in the treated POME and lower the stipulated discharge limits assigned by DoE, Malaysia, so that it conserves environmental pollution and preserves aquatic lives [7].

The biological treatment process is the most common wastewater treatment process employed by the Malaysian palm oil industry [2,8,9]. The distinct advantages of the biological treatment process are that the process can handle a large volume of wastewater, easy to operate, is effective in removing organic pollutants, cost-effective and eco-friendly [4,5,8,9]. Although the biological treatment process is considered promising for POME, the residual organic pollutants concentration in treated POME, in particular, the residual SS, BOD, and COD contractions, are upper than the release limits set by DOE, Malaysia [5,8]. Therefore, the biologically treated POME requires trained personnel to operate and urges for the post-treatment to comply with the recommended release limits set by DoE, Malaysia, before discharging into a watercourse. Several innovative technologies have been implemented as POME polishing or post-treatment technologies to minimize residual pollutant concentration in the biologically treated POME. Some of these methods include membrane technology [10], adsorption [11], photo catalysis [12], electrocoagulation [13], electrocoagulation–peroxidation [14] and coagulation–flocculation [15]. The coagulation–flocculation is considered as the most promising technology for the post-treatment of POME because of its numerous advantages, including simplicity in operation, low cost, effective in the elimination of colloidal and suspended organic particles [13,15]. However, the coagulation–flocculation process is always conducted using commercially obtainable inorganic coagulants, such as aluminum salt or iron (III) salt and poly aluminum chloride (PAC) [12,14,15]. Although alum-based commercial coagulant and polymeric coagulant have been found effective in POME polishing, the sludge generated from this process is classified as schedule waste by DOE, Malaysia, requiring costly disposal [14,16]. Thus, it urges determining alternative coagulants that can be utilized at equivalent coagulant efficiency with minimal treatment costs.

Iron (II) sulfate monohydrate ($FeSO_4 \cdot H_2O$) is an industrial by-product of the titanium processing industry [15,17,18]. Generally, a massive amount of ferrous sulfate heptahydrate ($FeSO_4 \cdot 7H_2O$) is produced throughout the manufacturing of TiO_2 from ilmenite or titanium slug using the sulfate process [17,19]. Subsequently, $FeSO_4 \cdot H_2O$ is produced from $FeSO_4 \cdot 7H_2O$ by heating the $FeSO_4 \cdot 7H_2O$ over 65 °C. The detailed chemical reaction for the production of $FeSO_4 \cdot H_2O$ is shown in Equation (1) to Equation (3).

$$FeTiO_3 + 2H_2SO_4 \rightarrow TiOSO_4 + FeSO_4 + 2H_2O \quad (1)$$

$$FeSO_4 + 7H_2O \rightarrow FeSO_4 \cdot 7H_2O \quad (2)$$

$$FeSO_4 \cdot 7H_2O \xrightarrow{\Delta} FeSO_4 \cdot H_2O + 6H_2O \quad (3)$$

The $FeSO_4 \cdot H_2O$ has been utilized as a coagulant for the elimination of hexavalent chromium [Cr(VI)] from industrial [19] effluent and as a redox-active metabolite for treating iron deficiency in plants [20]. The further utilization of $FeSO_4 \cdot H_2O$ as a coagulant for treating industrial effluent, such as POME, would enrich the sustainable deployment of

an industrial by-product. Additionally, it will determine an eco-friendly coagulant as a replacement for commercial coagulants for treating industrial effluent.

Several variables may potentially influence the $FeSO_4 \cdot H_2O$ coagulation efficiency for the removal of COD, SS, and BOD from POME. In the conventional approach of coagulation–flocculation experiments, it was determined the influence of one variable at a time, where other variables remained constant [14,21]. Therefore, some important aspects, such as interaction effects and quadratics effects of the variable are missing during the coagulation–flocculation process of POME, which contributes to the removal of COD, BOD, and SS from POME. The response surface methodology (RSM) is a combination of statistical mathematical techniques to determine the response of variables with considering the interaction and quadratics effects of the other variables [22,23]. In addition, RSM is an effective tool to optimize the experimental conditions of a process with minimal experimental runs [23]. In the present study, the $FeSO_4 \cdot H_2O$ waste was employed as a coagulant to eliminate SS, BOD, and COD from anaerobically treated POME. The emphasis was given to comply the residual contaminant concentrations in treated POME with the stringent discharge limits assigned by DoE, Malaysia. The effectiveness of the $FeSO_4 \cdot H_2O$ coagulation–flocculation was assessed with varying pH, coagulant doses, slow mixing speed, and flocculation time. The experimental conditions of the $FeSO_4 \cdot H_2O$ coagulation–flocculation were optimized using RSM to obtain maximum SS, COD, and BOD elimination from POME. The kinetics behavior and thermodynamics properties of $FeSO_4 \cdot H_2O$ waste as a coagulant were also determined for the elimination of SS, COD, and BOD from POME. Finally, the coagulation efficiency of $FeSO_4 \cdot H_2O$ waste was determined by characterizing $FeSO_4 \cdot H_2O$ waste and generated sludge using SEM, SEM-EDX, and FTIR. The results obtained in the present study will define an effective coagulant to replace the commercial coagulant for treating industrial effluents.

2. Materials and Methods

2.1. Experimental Procedure of Coagulation–Flocculation

The biologically treated tertiary POME was supplied by Sime Darby Plantation Sdn Bhd, Selangor, Malaysia. In the present study, the coagulation–flocculation experiments were conducted using jar test apparatus. The experiments were conducted following the standard methods of the coagulation–flocculation process of American Public Health Association (APHA) [18]. The influence of the $FeSO_4 \cdot H_2O$ coagulation–flocculation was measured on SS, COD and BOD elimination from POME with varying coagulant doses (1.0–2.0 g/L), pH (4–6), flocculation time (30–60 min) and slow mixing speed (20–50 rpm) at fixed rapid mixing for 3 min (200 rpm) and sedimentation time of 1 h. The percentage SS, COD, and BOD elimination from POME was computed using Equation (4).

$$\text{Removal } (\%) = \left(1 - \frac{C_t}{C_i}\right) \times 100 \quad (4)$$

where C_i and C_t denote the concentrations of SS, COD, and BOD at the initial (before treatment) and at the time "t" (after treatment), respectively.

2.2. Design of Experiments

The coagulation–flocculation experimental conditions were optimized using RSM to obtain the maximum elimination of SS, COD, and BOD from POME. The coagulation–flocculation experiments were designed using a central composite design (CCD) of experiments at two levels and four independent variables for the elimination of COD (Y_{COD}), BOD (Y_{BOD}), and SS (Y_{SS}). The independent variables were pH (X_1), coagulant doses (X_2), slow mixing speed (X_3), and flocculation time (X_4). A total of 30 sets of experimental runs were obtained from CCD, including 16 cube points, 8 axial points, and 6 center points. The regression coefficients among the variables were also generated on the COD (Y_{COD}), BOD (Y_{BOD}), and SS (Y_{SS}) elimination. The low, intermediate, and high levels of each variable

are depicted in Table 1. The percentage SS, COD, and BOD elimination was determined with the second-order polynomial equation, as revealed in Equation (5).

$$Y = B_o + \sum_{i=1}^{n} B_i X_i + \sum_{ipj}^{n} B_{ij} X_i X_j + \sum_{i=1}^{n} B_{ii} X_i^2 \quad (5)$$

where Y refers to the estimated response for the Y_{COD}, Y_{BOD}, and Y_{SS} elimination from POME using $FeSO_4 \cdot H_2O$ as a coagulant. B_0, B_i, B_{ij}, and B_{ii} represent the regression coefficient, "n" is the number of coded variables, X_iX_j represents independent variables. The Design Expert software was used to determine the goodness of fit of the experimental data with the predicted values obtained from the second-order polynomial equation. The significance of the independent variables for SS, COD, and BOD elimination from POME was predicted using the analysis of variance (ANOVA) analyses at a 95% ($p < 0.05$) confidence level. The adjusted coefficient of determination (R^2_{adj}) and coefficient of determination (R^2) was employed to determine the accuracy of the regression model. Three-dimensional response surface plots were utilized to present the interaction effects between the independent variables.

Table 1. The coded and uncoded level of the independent variables for S.S., COD, and BOD removal from POME using $FeSO_4 \cdot H_2O$ as a coagulant.

Independent Factors	Units	Symbol	Coded Levels		
			Low (−1)	Intermediate (0)	High (+1)
pH		x_1	4	5	6
Coagulant dosage	g/L	x_2	1.0	1.5	2.0
Slow mixing speed	rpm	x_3	20	35	50
Flocculation time	min	x_4	30	45	60

2.3. Kinetics and Thermodynamics Modeling

The kinetics and thermodynamics studies for SS, COD, and BOD elimination from the tertiary POME is crucial to determine the pollutant uptake rate, adsorption behavior, and thermodynamics behavior of the $FeSO_4 \cdot H_2O$ as a coagulant. The kinetics and thermodynamics studies of the $FeSO_4 \cdot H_2O$ coagulation for SS, COD, and BOD elimination from POME were carried with varying temperatures from 30–80 °C at a constant pH of 4.7, $FeSO_4 \cdot H_2O$ doses of 1.82 g/L, the rapid mixing time of 3 min, flocculation time of 60 min and slow mixing speed of 30 rpm. The kinetics behavior of $FeSO_4 \cdot H_2O$ coagulation efficiency was employed by implementing the pseudo-1st-order and pseudo-2nd-order kinetics model equation, as depicted in Equations (6) and (7), respectively [24].

$$\ln(q_e - q_t) = \ln q_e - k_1 t \quad (6)$$

$$\frac{t}{q_t} = \frac{1}{k_2 q_e^2} + \frac{t}{q_e} \quad (7)$$

where, q_t and q_e signify the elimination efficiency of SS, BOD, and COD from POME using $FeSO_4 \cdot H_2O$ as a coagulant at time "t" and equilibrium. In addition, k_1 and k_2 refer to the coagulation rate constant for the pseudo-1st-order and pseudo-2nd-order kinetics models, respectively. The thermodynamic properties, such as changes in enthalpy (ΔH^o), changes in entropy (ΔS^o), and the changes in Gibbs free energy, were determined using Equation (8) to Equation (10) [25].

$$\Delta G^o = -RT \ln K_o \quad (8)$$

$$\Delta G^o = -\Delta H^o - T\Delta S^o \quad (9)$$

$$\ln K_o = \frac{\Delta S^o}{R} - \frac{\Delta H^o}{RT} \quad (10)$$

where T denotes the kelvin temperature, R denotes the ideal gas constant (8.314 J/K. mole). The K_o was determined from the ratio between q_e and Ce. In addition, ΔS^o and ΔH^o values were evaluated from the intercept and slope of the plot $1/T$ vs. lnK_o.

2.4. Characterization

The pH of POME in treated and untreated POME was determined using a pH meter (Mettler Toledo F20). Concentrate sulfuric acid (1M) and sodium hydroxide (1M) solutions were employed to amend the desired pH of the solutions. The BOD (mg/L) concentration was determined using the HACH respirometric method of 10,099. Ten milliliters of untreated or treated POME were taken into the BOD track sample bottle and filled with deionized water. Consequently, BOD nutrient buffer pillow and lithium hydroxide powder pillow were taken into the BOD reagent bottle and stirred prior to incubating in a BOD track incubator at 20 °C for 5 days. The COD concentration was conducted using a HACH DR 2800 spectrometer. Two milliliters of homogenized POME and two milliliters of deionized water were taken into high range (HR) COD digestion vials (range 20 to 1500 mg/L) for sample and blank test, respectively. Then, the COD digestion vials were taken into the COD reactor and heated at 150 °C for 2 h. Later, the COD digestion vials were cooled to 120 °C and the COD (mg/L) was measured using a DRB 200 reactor. The SS concentration in untreated and treated POME was evaluated by employing the photometric method (HACH method 8006). A sample cell contains 10 mL of blended untreated and treated POME was taken in the sample cell holder and the SS concentration in untreated and treated POME were determined using a spectrophotometer (HACH DR 2800).

The chemical compositions in $FeSO_4 \cdot H_2O$ waste and sludge generated after coagulation of POME ($FeSO_4 \cdot H_2O$ sludge) were analyzed using Fourier transform infrared spectroscopy (FTIR) at a wavenumber of 600–4000 1/cm, scanning speed of 20 mm/s and 32 scans. The morphological changes in $FeSO_4 \cdot H_2O$ and $FeSO_4 \cdot H_2O$ sludge were determined using SEM image analyses at an accelerating voltage of 5 kV. The elemental compositions in $FeSO_4 \cdot H_2O$ and $FeSO_4 \cdot H_2O$ sludge were determined using SEM-EDX analyses.

3. Results and Discussion

3.1. Regression Model of Response

The initial pH, COD, BOD, and SS concentrations in tertiary POME were 8.5 ± 1, 3880 ± 7 mg/L, 194 ± 2 mg/L, and 933 ± 4 mg/L, respectively. The coagulation–flocculation experimental conditions were designed using CCD to eliminate SS, COD, and BOD from POME using $FeSO_4 \cdot H_2O$ as a coagulant. It obtained 30 experimental runs, consisting of 16 factorial runs, 6 center points, and 6 axial points. The RSM was applied to optimize the coagulation–flocculation experimental conditions to obtain maximum SS, COD, and BOD elimination from POME using $FeSO_4 \cdot H_2O$ as a coagulant. Table 2 summarizes the CCD of experiments of the independent variables for SS, COD, and BOD elimination from POME. The valuation of the regression coefficients for the SS, COD, and BOD elimination is presented in Table 3. The least square method was employed to determine the interaction effect between the variables, regression coefficients of intercept, linear effects of the variables, and quadratic effects of the variables. The significant and insignificant levels of the variables were assessed at $\alpha = 0.05$. Results show that pH, coagulant doses, and flocculation time significantly affect the elimination of SS, COD, and BOD elimination from POME using $FeSO_4 \cdot H_2O$ as a coagulant. The slow mixing speed had an insignificant effect on the COD and BOD removal, showing a significant effect on SS removal. The predicted values for the elimination of COD, BOD, and SS were calculated by employing the second-order polynomial equation, as depicted in Equation (11), Equation (12), and Equation (13), respectively.

$$\begin{aligned} Y_{COD} = 95.926 - 4.661x_1 - 3.053x_2 - 0.666x_3 + 5.526x_4 - 11.443{x_1}^2 - 4.763{x_2}^2 - 3.736{x_3}^2 - 2.260{x_4}^2 \\ + 0.534x_1x_2 + 0.249x_1x_3 - 1.41x_1x_4 + 0.239x_2x_3 + 0.05x_2x_4 - 0.48x_3x_4 \end{aligned} \quad (11)$$

$$Y_{BOD} = 94.47 - 2.416x_1 + 5.799x_2 - 0.261x_3 + 3.327x_4 - 12.643{x_1}^2 - 6.34{x_2}^2 - 1.975{x_3}^2 - 2.889x_1x_2 - 0.409x_1x_3 + 1.474x_1x_4 + 1.534x_2x_3 + 0.724x_2x_4 - 0.066x_3x_4 \quad (12)$$

$$Y_{ss} = 95.209 - 2.614x_1 + 4.949x_2 - 1.461x_3 + 3.444x_4 - 9.645{x_1}^2 - 1.012{x_2}^2 - 7.042{x_3}^2 - 0.467{x_4}^2 - 1.042x_1x_2 - 0.198x_1x_3 + 0.01x_1x_4 + 0.37x_2x_3 - 0.137x_2x_4 - 0.895x_3x_4 \quad (13)$$

where Y_{COD}, $Y_{BOD,}$ and Y_{SS} are the responses for COD, BOD, and SS elimination from POME using $FeSO_4 \cdot H_2O$ as a coagulant, respectively. The predicted values were compared with the experimental values for the elimination of SS, COD, and BOD from POME, which was found to be a good fit between the actual and predicted data (Table 2). Table 4 shows ANOVA analyses for SS, COD, and BOD elimination from POME. The term "lack of fit" indicates the aptness of the regression model to predict the response within levels of the variables studied. A significant lack of fit of a regression model reveals the inappropriate prediction of the response by the proposed regression model. The total deviation from the anticipated response is specified by the coefficient of determination (R^2). The ratio of the sum of squares attributable to the regression to the entire sum of squares is expressed by the R^2 measurement. The proximity of R^2 to the value of 1 serves as a measure of the adequacy of the regression model prediction. The level of influence of the independent variables in predicting the response is determined by the R^2 value. The R^2 and R^2_{adj} values for COD, BOD, and SS were found to be 0.9859, 0.9718, 0.9870, 0.974, and 0.9955, 0.991, respectively, illuminating the high correlation between anticipated data and experimental data for the elimination of SS, COD, and BOD from POME using $FeSO_4 \cdot H_2O$ as a coagulant. In addition, the ANOVA analysis showed that the lack of fit was insignificant, which implies that experimental data adequately fitted the proposed second-order polynomial equation to describe the SS, COD, and BOD elimination from POME using $FeSO_4 \cdot H_2O$ as a coagulant. The R^2 and R^2 (adj) values, as well as the insignificant lack of fit, imply the regression model's suitability for predicting the response within the level of the variable studies [26,27].

Table 2. The central composite design of experiments for the removal of COD, BOD, and SS from POME using $FeSO_4 \cdot H_2O$ as a coagulant.

Run	X_1	X_2	X_3	X_4	Removal (%)					
					COD		BOD		SS	
					Observed	Predicted	Observed	Predicted	Observed	Predicted
1	4	1	20	30	64.46	68.48	64.59	64.13	71.28	72.57
2	6	1	20	30	60.87	60.41	63.32	62.94	69.86	69.8
3	4	2	20	30	72.67	72.94	76.89	76.99	85.46	84.08
4	6	2	20	30	68.6	67.01	64.43	64.25	76.91	77.15
5	4	1	50	30	67.61	67.13	61.62	61.49	70.63	71.09
6	6	1	50	30	58.59	60.06	60.28	58.67	67.58	67.53
7	4	2	50	30	71.95	72.55	78.41	80.48	84.26	84.09
8	6	2	50	30	66.18	67.61	66.38	66.11	75.28	76.36
9	4	1	20	60	84.94	83.21	66.31	66.52	82.92	81.5
10	6	1	20	60	69.26	69.51	72.28	71.23	78.46	78.77
11	4	2	20	60	88.5	87.87	79.64	82.27	92.28	92.47
12	6	2	20	60	76.12	76.3	75.36	75.43	86.37	85.57
13	4	1	50	60	77.51	79.95	62.41	63.61	76.54	76.44
14	6	1	50	60	67.8	67.23	66.85	66.69	71.89	72.92
15	4	2	50	60	85.4	85.56	85.19	85.5	89.17	88.89
16	6	2	50	60	78.16	74.98	75.54	77.02	82.35	81.2
17	5	1.5	35	45	96.5	94.75	91.42	93.13	96.34	96.94

Table 2. *Cont.*

Run	X_1	X_2	X_3	X_4	Removal (%)					
					COD		BOD		SS	
					Observed	Predicted	Observed	Predicted	Observed	Predicted
18	5	1.5	35	45	96.5	94.75	96.83	93.13	97.69	96.94
19	5	1.5	35	45	93.1	94.75	91.26	93.13	95.99	96.94
20	5	1.5	35	45	95.1	94.75	96.84	93.13	96.92	96.94
21	3	1.5	35	45	62.7	60.65	52.55	50.06	59.52	60.13
22	7	1.5	35	45	40.5	42	38.87	40.4	50.07	49.67
23	5	0.5	35	45	74.14	71.94	57.17	58.84	80.36	79.53
24	5	2.5	35	45	82.5	84.15	84.67	82.04	98.29	99.33
25	5	1.5	5	45	83.37	83.49	88.41	88.42	67.51	68.23
26	5	1.5	65	45	81.49	80.82	88.35	87.38	62.9	62.39
27	5	1.5	35	15	79.37	77.01	80.38	81.29	85.52	84.72
28	5	1.5	35	75	97.3	99.11	96.47	94.6	97.49	98.5
29	5	1.5	35	45	96.2	97.1	94.36	95.8	95.27	93.48
30	5	1.5	35	45	95.81	97.1	93.42	95.8	92.51	93.48

Table 3. The regression coefficient for the removal of SS, BOD and COD from POME using $FeSO_4 \cdot H_2O$ as a coagulant.

Term	Coefficient			Standard Error			*T*-Value			*p*-Value		
	COD	BOD	SS	COD	BOD	SS	COD	BOD	SS	COD	BOD	SS
Constant	95.926	94.47	95.209	0.978	1.01	0.506	98.07	93.09	188.14	0.000	0.000	0.000
X_1	−4.661	−2.416	−2.614	0.483	0.501	0.250	−9.65	−4.82	−10.46	0.000	0.000	0.000
X_2	3.053	5.799	4.949	0.483	0.501	0.250	6.32	11.57	19.80	0.000	0.000	0.000
X_3	−0.666	−0.261	−1.461	0.483	0.501	0.250	−1.38	−0.52	−5.85	0.190	0.611	0.000
X_4	5.526	3.327	3.444	0.483	0.501	0.250	11.44	6.64	13.78	0.000	0.000	0.000
X_1^2	−11.443	−12.643	−9.645	0.452	0.469	0.234	−25.33	−26.97	−41.26	0.000	0.000	0.000
X_2^2	−4.763	−6.340	−1.012	0.452	0.469	0.234	−10.54	−13.52	−4.33	0.000	0.000	0.001
X_3^2	−3.736	−1.975	−7.042	0.452	0.469	0.234	−8.27	−4.21	−30.12	0.000	0.001	0.000
X_4^2	−2.260	−1.964	−0.467	0.452	0.469	0.234	−5.00	−4.19	−2.00	0.000	0.001	0.066
X_1X_2	0.534	−2.889	−1.042	0.592	0.614	0.306	0.90	−4.71	−3.41	0.382	0.000	0.004
X_1X_3	0.249	−0.409	−0.198	0.592	0.614	0.306	0.42	−0.67	−0.65	0.681	0.516	0.529
X_1X_4	−1.410	1.474	0.010	0.592	0.614	0.306	−2.38	2.40	0.03	0.032	0.031	0.974
X_2X_3	0.239	1.534	0.370	0.592	0.614	0.306	0.40	2.50	1.21	0.693	0.026	0.247
X_2X_4	0.050	0.724	−0.137	0.592	0.614	0.306	0.08	1.18	−0.45	0.934	0.258	0.660
X_3X_4	−0.480	−0.066	−0.895	0.592	0.614	0.306	−0.81	−0.11	−2.92	0.431	0.916	0.011

Table 4. Analysis of variance (ANOVA) for the regression model for the removal of SS, BOD and COD from POME using $FeSO_4 \cdot H_2O$ as a coagulant.

Source	Degree of Freedom	Sum of Squares			Mean Square			*F*-Value			*p*-Value		
		[a] COD	[b] BOD	[c] SS	COD	BOD	SS	COD	BOD	SS	COD	BOD	SS
Block	1	36.72	47.62	80.04	36.72	47.62	80.04						
Model	14	5479.52	6399.73	4668.36	391.39	457.12	333.45	69.89	75.83	222.45	<0.0001	<0.0001	<0.0001
Residual	14	78.40	84.40	20.99	5.60	6.03	1.50						
Lack of fit	10	70.56	53.75	15.52	7.06	5.37	1.55	3.60	0.7014	1.14	0.1142	0.7051	0.4907
Pure error	4	7.84	30.65	5.47	1.96	7.66	1.37						
Total	29	5594.64	6531.74	4769.39									

[a] $R^2 = 0.9859$; $R^2_{(adj)} = 0.9718$. [b] $R^2 = 0.9870$; $R^2_{(adj)} = 0.9740$. [c] $R^2 = 0.9955$; $R^2_{(adj)} = 0.9910$.

The least squares methods used to create residual plots for evaluating the regression model's adequacy for COD, BOD, and SS elimination are shown in Figure 1. The standard plots of the residual plots and the link between the normal percentage probabilities and the studentized residual produced demonstrate that the residual distributions are adequately expressed by the normal distribution as given for the independent variables. The residual plots exhibit linear behavior, as a straight line is formed, indicating that the predictions of the suggested models are valid [24,28]. The R^2 and R^2 (adj) values obtained in the present study suggest that the model suitably expressed the coagulation process for the SS, COD, and BOD elimination from POME using $FeSO_4 \cdot H_2O$ as a coagulant.

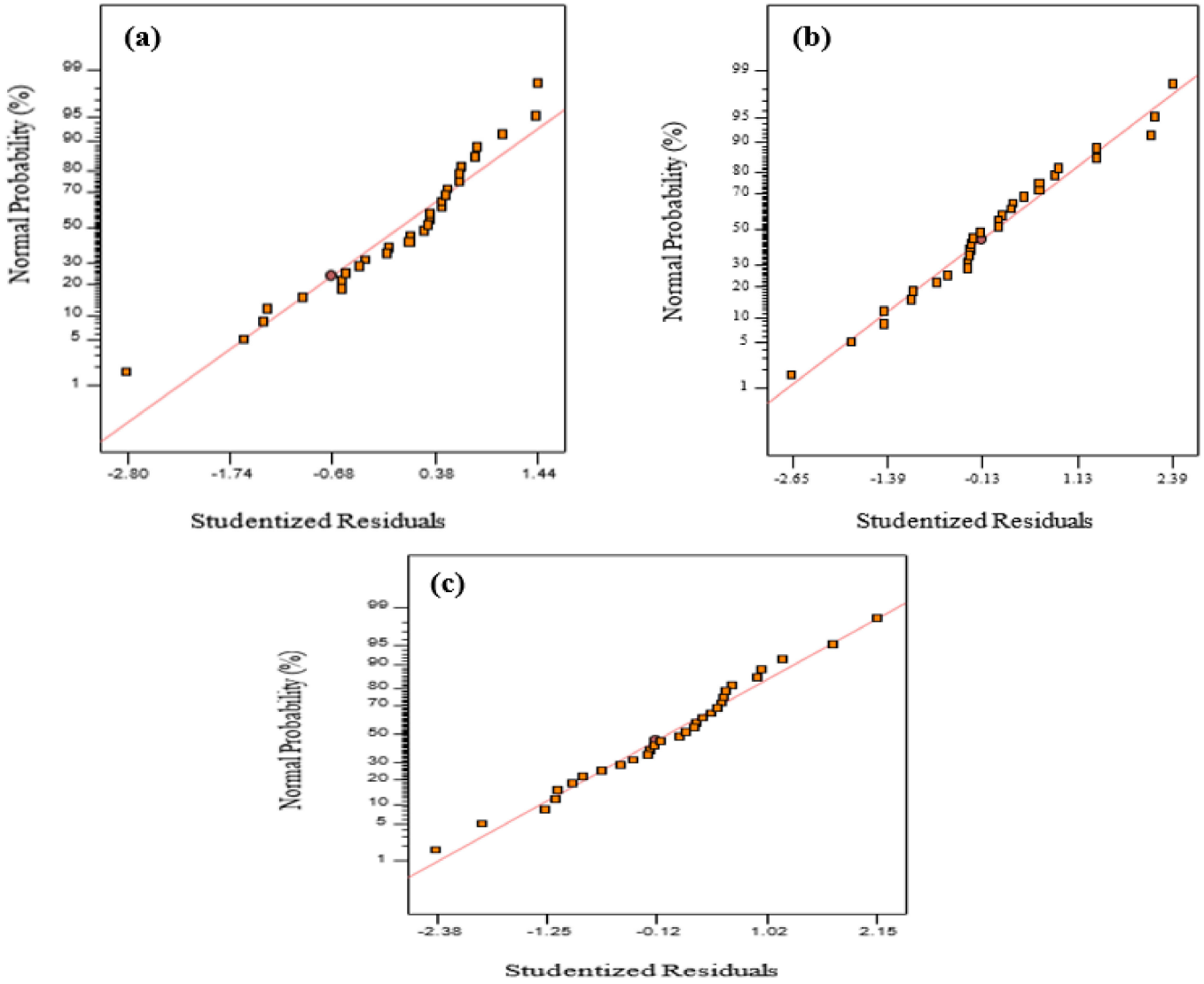

Figure 1. Normal probability plot versus studentized residual of the second-order quadratic model (**a**) SS removal (**b**) BOD removal (**c**) COD elimination.

3.2. Response Surface Analyses

Figure 2 shows the three-dimensional surface plots of the interaction effect between pH and $FeSO_4 \cdot H_2O$ doses (Figure 2a), slow mixing speed and pH (Figure 2b), pH and flocculation time (Figure 2c), coagulant doses, and slow mixing speed (Figure 2d), coagulant doses and flocculation time (Figure 2e), and slow mixing speed and flocculation time (Figure 2f) for percentage elimination of COD from POME. It was observed that the interaction effect between flocculation time and pH was statistically significant to eliminate COD from POME. Conversely, the interaction effect between pH and $FeSO_4 \cdot H_2O$ doses (Figure 2a), pH and slow mixing speed (Figure 2b), $FeSO_4 \cdot H_2O$ doses and slow mixing speed (Figure 2d), $FeSO_4 \cdot H_2O$ doses and flocculation time (Figure 2e), and slow mixing speed and flocculation time (Figure 2f) were statistically insignificant for the elimination of COD in POME. It was found that the percentage of COD elimination increased when pH increased from 4 to 5 and decreased from 5 to 6 as the coagulant doses, flocculation speed, and flocculation time increased, respectively. The interaction between coagulant doses with slow mixing speed (Figure 2d) showed that the percentage of COD elimination increased when coagulant doses and slow mixing speed increased. The percentage of COD elimination started to become persistent when the slow mixing speed was above 30 rpm and slightly decreased until it reached 50 rpm. Figure 2e shows the interaction between coagulant doses and flocculation time, revealing that the COD elimination from POME enhanced with increasing $FeSO_4 \cdot H_2O$ doses at a higher flocculation time until 1.8 g/L coagulant doses; consequently, the COD elimination was negligible with further increase in $FeSO_4 \cdot H_2O$ doses. The interaction between slow mixing speed and flocculation time (Figure 2f) shows that the COD elimination percentage increased as the interactional factors increased. Over 90% elimination of COD in POME was achieved at pH 5, coagulant doses 1.5 g/L, slow mixing speed 35 rpm, and flocculation time 45 min.

Figure 3 shows the three-dimensional surface plot on the interaction effect between pH and coagulant doses (Figure 3a), pH and slow mixing speed (Figure 3b), pH and flocculation time (Figure 3c), $FeSO_4 \cdot H_2O$ doses, and slow mixing speed (Figure 3d), $FeSO_4 \cdot H_2O$ doses and flocculation time (Figure 3e), and slow mixing speed and flocculation time (Figure 3f) for the BOD elimination from POME. It was perceived that the interaction effect between pH and $FeSO_4 \cdot H_2O$ doses (Figure 3a), pH and flocculation time (Figure 3c), and $FeSO_4 \cdot H_2O$ doses and slow mixing speed (Figure 3d) was statistically significant for the BOD elimination from POME. The interaction effect between pH and slow mixing speed (Figure 3b), coagulant doses and flocculation time (Figure 3e), and slow mixing speed and flocculation time (Figure 3f) were insignificant for the elimination of COD in POME. The percentage of BOD removed (over 90%) with increasing pH from 4 to 5 and decreased after pH 5 with increasing coagulant doses, flocculation speed, and flocculation time. Figure 3d illustrates the interaction effect between slow mixing speed and coagulant doses. It shows that the percentage of BOD elimination increased as coagulant doses and slow mixing speed increased. The highest elimination of BOD was about 92% at pH 5 and flocculation time 45 min. Similarly, the interaction effect between flocculation time and coagulant doses (Figure 3e) reveals an increase in BOD elimination in POME as the coagulant doses and flocculation time increased. Nevertheless, as the interaction between slow mixing speed and flocculation time increased (Figure 4f), it showed negligible BOD removal. Approximately 96% BOD elimination was obtained at $FeSO_4 \cdot H_2O$ doses of 2 g/L, pH 5, slow mixing speed of 35 rpm, and flocculation time of 60 min.

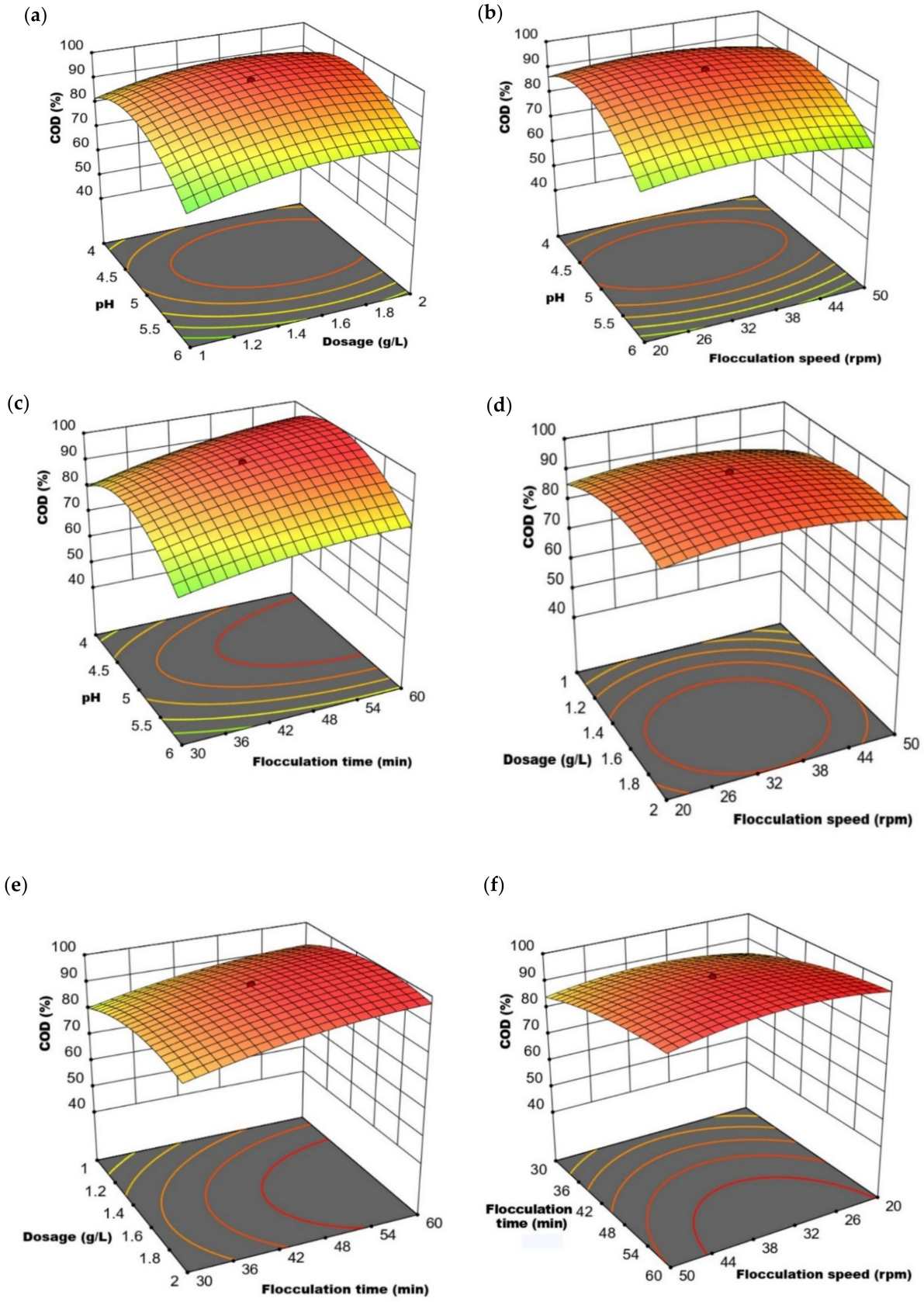

Figure 2. Interaction effects between independent variable for the COD elimination from POME using $FeSO_4 \cdot H_2O$ as coagulant. (**a**) Between pH and coagulant doses, (**b**) between pH and flocculation speed, (**c**) between pH and flocculation time, (**d**) between coagulant doses and flocculation speed, (**e**) between coagulant doses and flocculation time, (**f**) between slow mixing speed and flocculation time.

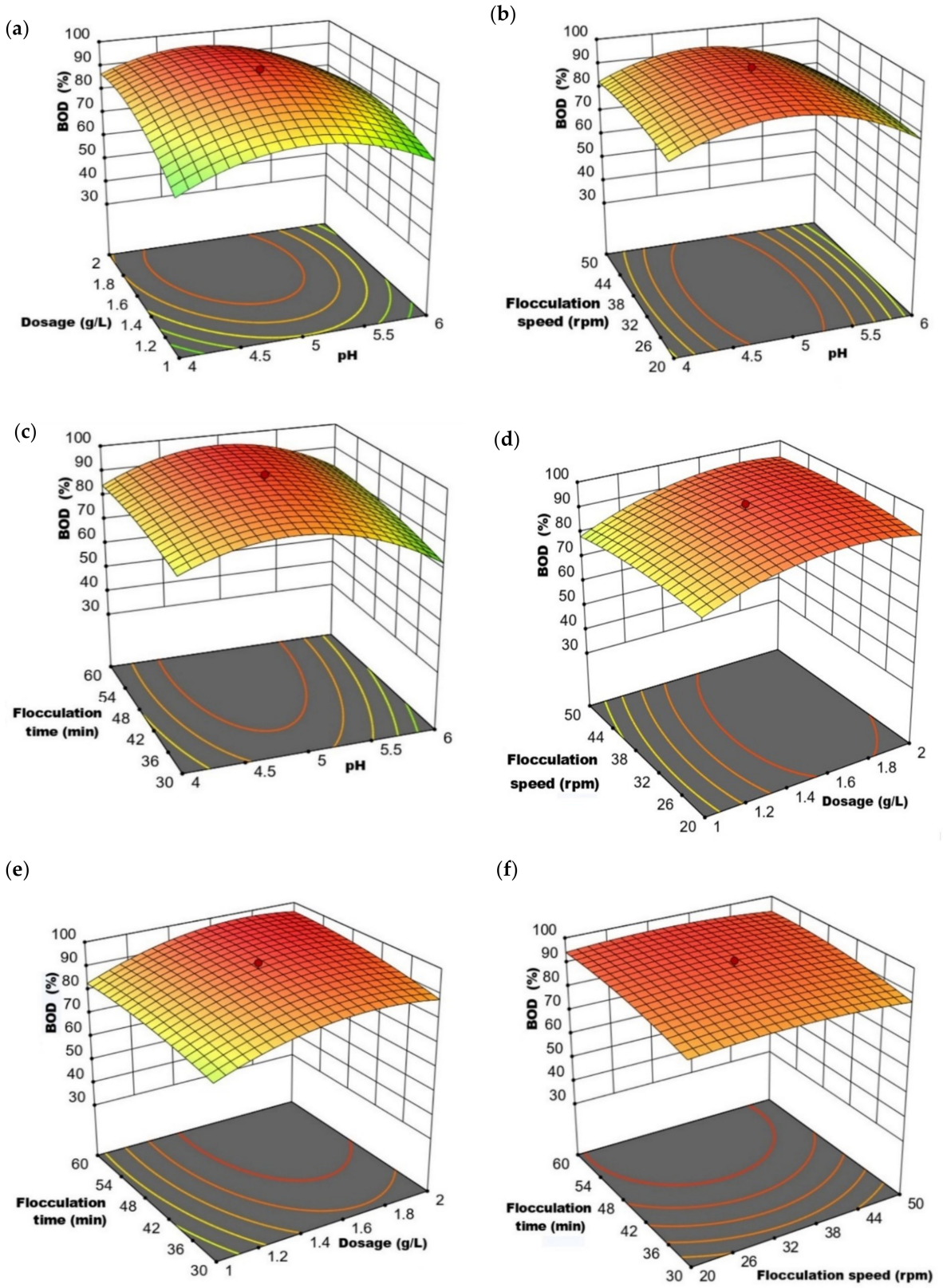

Figure 3. Interaction effects between independent variable for the BOD elimination from POME using $FeSO_4 \cdot H_2O$ as coagulant. (**a**) Between pH and coagulant doses, (**b**) between pH and flocculation speed, (**c**) between pH and flocculation time, (**d**) between coagulant doses and flocculation speed, (**e**) between coagulant doses and flocculation time, (**f**) between slow mixing speed and flocculation time.

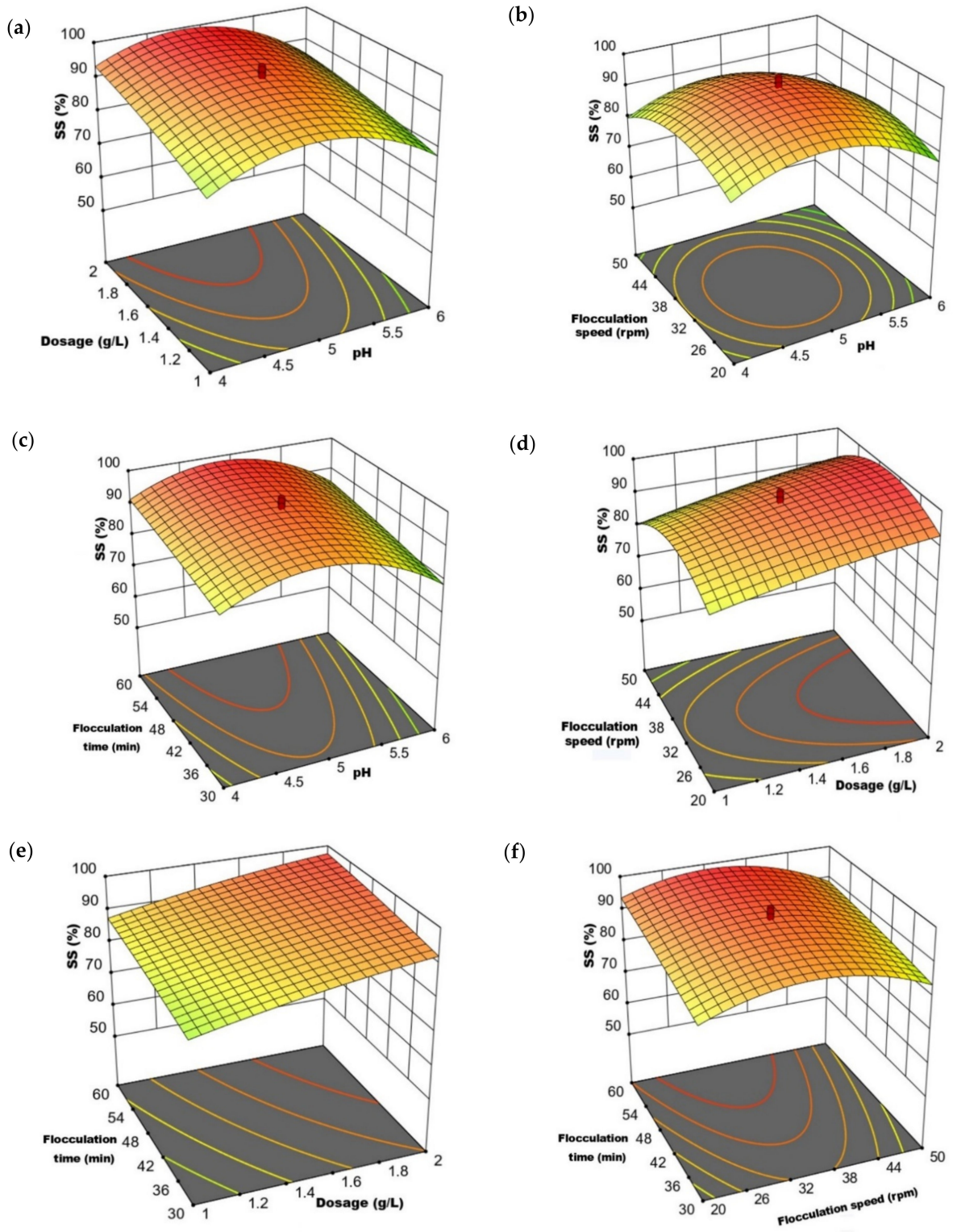

Figure 4. Interaction effects between independent variable for the SS elimination from POME using $FeSO_4 \cdot H_2O$ as coagulant. (**a**) Between pH and coagulant doses, (**b**) between pH and flocculation speed, (**c**) between pH and flocculation time, (**d**) between coagulant doses and flocculation speed, (**e**) between coagulant doses and flocculation time, (**f**) between slow mixing speed and flocculation time.

The three-dimensional surface plots in Figure 4 show the interaction effect between pH and $FeSO_4 \cdot H_2O$ doses (Figure 4a), pH and slow mixing speed (Figure 4b), pH and flocculation time (Figure 4c), coagulant doses, and slow mixing speed (Figure 4d), coagulant doses and flocculation time (Figure 4e), and slow mixing speed and flocculation time (Figure 4f) for percentage elimination of SS from POME. The interaction effect between $FeSO_4 \cdot H_2O$ doses and pH (Figure 4a) and slow mixing speed and flocculation time (Figure 4f) were statistically significant for the elimination of SS from POME. The interaction between pH and slow mixing speed (Figure 4b), pH and flocculation time (Figure 4c), coagulant doses and slow mixing speed (Figure 4d), and coagulant doses and flocculation time (Figure 4e) were insignificant for the COD elimination from POME. As illustrated in Figure 4a,c, the percentage of SS elimination was increased as the pH increased from 4 to 5 and declined as the coagulant doses and flocculation time increased after pH 5. From Figure 4a,b, the highest SS elimination was obtained at about 99% and 98% at pH 4.7, coagulants dose 2 g/L, slow mixing speed at 35 rpm, flocculation time 45 min and pH 4.7, coagulant doses 1.5 g/L, slow mixing speed 35 rpm, flocculation time 60 min, respectively. The decrease in the SS elimination from POME might be due to the weaker interaction between pH and flocculation speed. Figure 4d represents the interaction effect between slow mixing speed and $FeSO_4 \cdot H_2O$ doses. The percentage of SS elimination was improved with an increasing slow mixing speed at higher coagulants doses until 35 rpm of flocculation speed; wherein, the percentage of SS elimination was negligible with the elevated slow mixing speed over 35 rpm. The maximum SS elimination of about 99% was obtained at $FeSO_4 \cdot H_2O$ doses 2 g/L, pH 5, slow mixing speed 35 rpm, and flocculation time 45 min. Figure 4e revealed that the SS elimination increased with increasing $FeSO_4 \cdot H_2O$ doses at higher flocculation time. Similarly, the SS elimination increased with increasing flocculation time at higher $FeSO_4 \cdot H_2O$ doses. The optimal, about 98% of SS elimination, was obtained at the $FeSO_4 \cdot H_2O$ doses of 2g/L, flocculation time of 60 min, slow mixing speed of 35 rpm and pH 5. Figure 4f shows the interaction effect between slow mixing speed and flocculation time for the SS elimination from POME. It was perceived that the SS elimination increased with elevated slow mixing speed from 20 rpm to 30 rpm at a higher flocculation time. Nonetheless, the increase in SS elimination was negligible with flocculation time at a higher flocculation speed. Over 90% of SS elimination was obtained at pH 5, coagulant doses 1.5 g/L, slow mixing speed 35 rpm, and flocculation time 45 min.

Both pH and $FeSO_4 \cdot H_2O$ doses had played a significant role in removing COD, BOD, and SS from POME using $FeSO_4 \cdot H_2O$ as a coagulant. The utmost coagulation competence at pH 5 can be described as the uppermost solubility of the iron (III) hydroxide and the maximum charge density in the acidic solution; as a result, the colloidal and suspended particles were accumulated on the surface of the coagulant by the charge-neutralizing processes [28]. Above pH 5.0, the $FeSO_4 \cdot H_2O$ coagulation effectiveness decreases because iron (III) hydroxide's slower solubility affects COD, BOD, and SS elimination [29,30]. The increased $FeSO_4 \cdot H_2O$ doses lead to an increase in coagulation efficiency with the higher amount of Fe(II) particles in the solution, which results in increased negatively charged organic particle neutralization and iron exchange with positively charged iron(II) particles to eliminate the pollutants [15,31]. The reduction in coagulation effectiveness of $FeSO_4 \cdot H_2O$ with increasing coagulant doses beyond 1.8 g/L might be explained by an increase in the surface zeta potential of suspended and colloidal particles [32,33].

3.3. Process Optimization and Validation

The design expert software (STAT EASE Inc., Minneapolis, U.S.) was utilized to optimize the $FeSO_4 \cdot H_2O$ coagulation–flocculation process to eliminate SS, BOD, and COD from POME. Table 5 shows the optimum experimental conditions for the SS, BOD, and COD elimination from POME using $FeSO_4 \cdot H_2O$ as a coagulant. It was found that the optimum coagulation–flocculation experimental conditions for the SS, BOD, and COD elimination from POME were pH 4.7, $FeSO_4 \cdot H_2O$ doses of 1.82 g/L, slow mixing speed of 30 rpm, and flocculation time 60 min. The maximum COD, BOD, and SS elimination

from POME obtained at the optimal experimental conditions of $FeSO_4 \cdot H_2O$ coagulation were 96.21%, 96.72%, and 96.97%, respectively. As can be seen in Table 5, the percentage of COD, BOD, and SS elimination was closer to the predicted responses, indicating that the second-order polynomial equation adequately determined the optimum experimental conditions of $FeSO_4 \cdot H_2O$ coagulation for the SS, BOD, and COD elimination. Similarly, Ngteni et al. [29] obtained over 95% of NH_3-N, 99% of SS, 97% of BOD, and 99% of COD elimination from secondary rubber processing wastewater (SRPW) using $FeSO_4 \cdot 7H_2O$ waste as a coagulant. Mohammad Illias et al. [24] effectively eliminated NH_3-N and COD from rubber processing effluent by employing $FeSO_4 \cdot 7H_2O$ waste as an environmentally friendly coagulant. Thus, it can be postulated that $FeSO_4 \cdot H_2O$ could be implemented in the post-treatment POME for the safe discharge of the treated effluent in the watercourse.

Table 5. Verification of optimum experimental condition for the removal of COD, BOD, and SS using $FeSO_4 \cdot H_2O$ as a coagulant.

Parameters	Optimized Condition	Removal (%)					
		COD		BOD		SS	
		Predicted	Actual	Predicted	Actual	Predicted	Actual
pH	4.7	97.73	96.21 ± 2.34	98.15	96.72 ± 1.85	97.58	96.97 ± 2.18
Coagulant dosage (g/L)	1.82						
Slow mixing speed (rpm)	30						
Flocculation time (min)	60						

3.4. Kinetics and Thermodynamics Modeling

The coagulation–flocculation mechanisms and mass transport phenomena of the $FeSO_4 \cdot H_2O$ were determined to eliminate SS, COD, and BOD from POME using pseudo-second-order kinetics and pseudo-first-order equations. Table 6 shows the kinetics properties of FeSO4·H2Ocoagulation for the SS, COD, and BOD elimination from POME. It was found that the $FeSO_4 \cdot H_2O$ coagulation competence (q_{exp}) to eliminate SS, COD, and BOD from POME increased with increasing coagulation temperature from ambient temperature (28 ± 1 °C) to 70 °C, indicating that the inclusion temperature enhanced the coagulation adeptness of $FeSO_4 \cdot H_2O$ to eliminate SS, COD, and BOD from POME. Similarly, Ngteni et al. [26] reported that the rise in $FeSO_4 \cdot 7H_2O$ coagulation temperature increased the NH_3-N SS, BOD, and COD elimination because of increasing collision between coagulant particles and suspended organic particles [26]. The correlation coefficient (R^2) values and differences between experimental coagulation efficiency values (q_{exp}) and theoretical coagulation efficiency values (q_{cal}) were evaluated to decide the well-described kinetics model equations for the SS, COD, and BOD elimination from POME. The R^2 values obtained from the pseudo-second-order kinetics equation ($R^2 > 0.99$) were closer to unity than the pseudo-first-order kinetics equation ($R^2 \leq 0.99$). In addition, the q_e (exp) values were much closer to the obtained q_e(cal) values from the pseudo-second-order kinetics equation than the q_e (cal) values of the pseudo-first-order kinetics equation. Thus, it can be determined that the pseudo-second-order kinetics equation best described the kinetics model for the elimination of SS, COD, and BOD from POME using $FeSO_4 \cdot H_2O$ as a coagulant. Wherein the chemisorption would be the possible coagulation–adsorption mechanism for the elimination of SS, COD, and BOD from POME using $FeSO_4 \cdot H_2O$ as a coagulant [24].

Table 6. Kinetics and thermodynamics modeling for the removal of COD, BOD, and SS from tertiary POME using $FeSO_4 \cdot H_2O$ as a coagulant.

Parameters	T (°C)	q_e (Exp) (mg/mg)	Pseudo-1st-Order Kinetics			Pseudo-2nd-Order Kinetics			Thermodynamics		
			q_e (mg/mg)	K_1 (1/min)	R^2	q_e (mg/mg)	K_2 (mg/mg.min)	R^2	ΔG^o (kJ/mol)	ΔH^o (kJ/mol)	ΔS^o (J/mol)
COD	28	1.519	1.466	0.0531	0.9711	1.731	0.076	0.9953	8.622	8.426	−5.372
	40	1.526	1.342	0.0524	0.9687	1.703	0.093	0.9984	8.628		
	50	1.530	1.096	0.0444	0.9553	1.666	0.123	0.9991	8.635		
	60	1.551	1.022	0.0375	0.9951	1.660	0.142	0.9993	8.641		
	70	1.562	1.155	0.0481	0.9598	1.651	0.162	0.9997	8.648		
BOD	28	0.767	0.746	0.0227	0.9987	0.854	0.148	0.9975	8.401	8.337	−1.758
	40	0.769	0.715	0.0217	0.9975	0.839	0.175	0.9955	8.403		
	50	0.771	0.686	0.0206	0.9864	0.841	0.183	0.9965	8.406		
	60	0.777	0.639	0.0173	0.9296	0.842	0.197	0.9971	8.408		
	70	0.778	1.306	0.0025	0.8981	0.830	0.240	0.9983	8.410		
SS	28	3.525	1.330	0.0019	0.9711	3.824	0.039	0.9953	8.675	8.419	−7.034
	40	3.545	1.452	0.0258	0.9774	3.848	0.041	0.9948	8.684		
	50	3.554	1.459	0.0316	0.9568	3.854	0.048	0.9965	8.692		
	60	3.579	1.462	0.0347	0.9746	3.864	0.054	0.9984	8.701		
	70	3.587	1.377	0.0364	0.9779	3.797	0.074	0.9995	8.709		

The thermodynamics properties, for example, the changes in Gibbs free energy (ΔG^o), changes in entropy (ΔS^o), changes in enthalpy (ΔH^o) were determined for the SS, COD, and BOD elimination from POME using $FeSO_4 \cdot H_2O$ as a coagulant, as shown in Table 6. The ΔG^o represents the spontaneity of the coagulation–flocculation process. It was found the ΔG^o values enhanced with increasing temperature for the SS, COD, and BOD elimination from POME using $FeSO_4 \cdot H_2O$ as a coagulant, which indicates that the external energy source influences the coagulation–flocculation efficiency [34]. The ΔG^o values for the SS, COD, and BOD elimination were determined within the range of 8.675–8.709 kJ/mol, 8.622–8.648 kJ/mol, and 8.401–8.410 kJ/mol, respectively. The positive ΔG^o values indicate that the coagulation–flocculation process for the SS, COD, and BOD elimination from POME was non-spontaneous. The ΔH^o values for the SS, COD, and BOD elimination were obtained to be 8.419 kJ/mol, 8.426 kJ/mol and 8.337 kJ/mol, respectively. The obtained positive ΔH^o values indicate that the $FeSO_4 \cdot H_2O$ coagulation–flocculation process was endothermic for the SS, COD, and BOD elimination from POME. The negative ΔS^o values for the SS (−7.034 kJ/mol), COD (−5.372 kJ/mol), and BOD (−1.758 kJ/mol) elimination indicate the decrease in entropy of the liquid–solid interface with increasing temperature during the coagulation–flocculation process for the elimination of SS, COD, and BOD from POME using $FeSO_4 \cdot H_2O$ as a coagulant.

3.5. Assessment Post-Treatment of POME Using $FeSO_4 \cdot H_2O$ as a Coagulant

The $FeSO_4 \cdot H_2O$ has a good coagulant efficiency because of the accompanying mechanism with the suspended and colloidal particles in the effluent [15,31]. Generally, the $FeSO_4 \cdot H_2O$ is partially hydrolyzed in an aqueous solution; therefore, it reduces the repulsion force between the colloidal particles by lessening the double diffusion layer of adjoining colloidal particles [31]. Figure 5 shows the SEM image of raw $FeSO_4 \cdot H_2O$

(Figure 5a) and the generated $FeSO_4 \cdot H_2O$ sludge after coagulation–flocculation of POME (Figure 5b). It was found that the surface of the raw $FeSO_4 \cdot H_2O$ exhibits voids, aligned, and well-diffused porous surfaces (Figure 5a). It was observed that the voids were absent on the surface of the iron sludge. This is because the voids were filled entirely due to the agglomeration of the suspended and colloidal organic particles with $FeSO_4 \cdot H_2O$ during the coagulation–flocculation process of POME (Figure 5b). Figure 6 shows the SEM-EDX spectra of raw $FeSO_4 \cdot H_2O$ (Figure 6a) and sludge generated after coagulation–flocculation of POME using $FeSO_4 \cdot H_2O$ as a coagulant (Figure 6b). The elemental composition analyses show the presence of Fe, S, O, and C in the SEM-EDX spectra of raw $FeSO_4 \cdot H_2O$ (Figure 6a). It was found that the SEM-EDX spectra show the presence of C, S, Fe, O, Si, S, and K in the sludge generated after the coagulation–flocculation of POME. These findings revealed that the $FeSO_4 \cdot H_2O$ effectively removed the suspended particles from POME during the coagulation–flocculation process. The $FeSO_4 \cdot H_2O$ coagulation efficiency could be attributed to the Fe^{2+} and sulfonic groups, which combined the collided and suspended organic and inorganic particles and thereby removed the SS, COD, and BOD from POME [35,36].

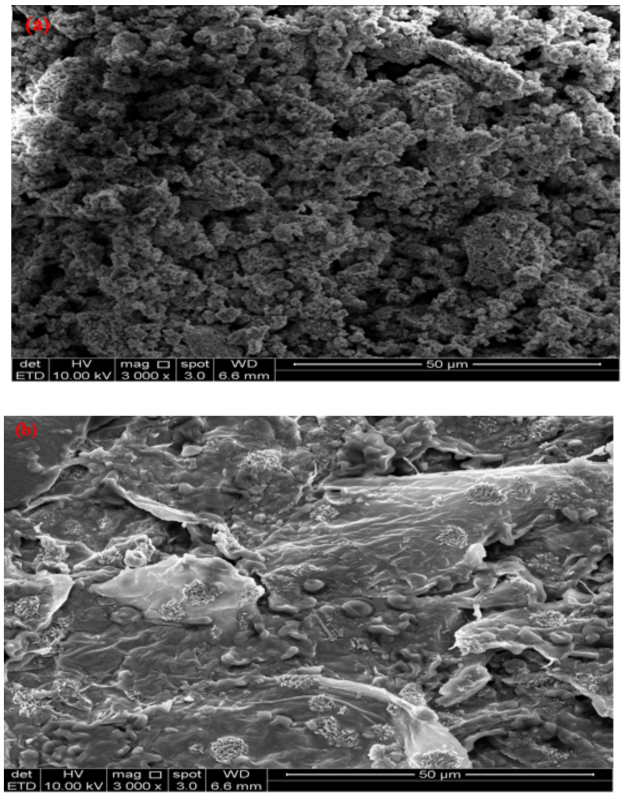

Figure 5. Scanning electron microscope image of (**a**) raw $FeSO_4 \cdot H_2O$, and (**b**) sludge generated after coagulation.

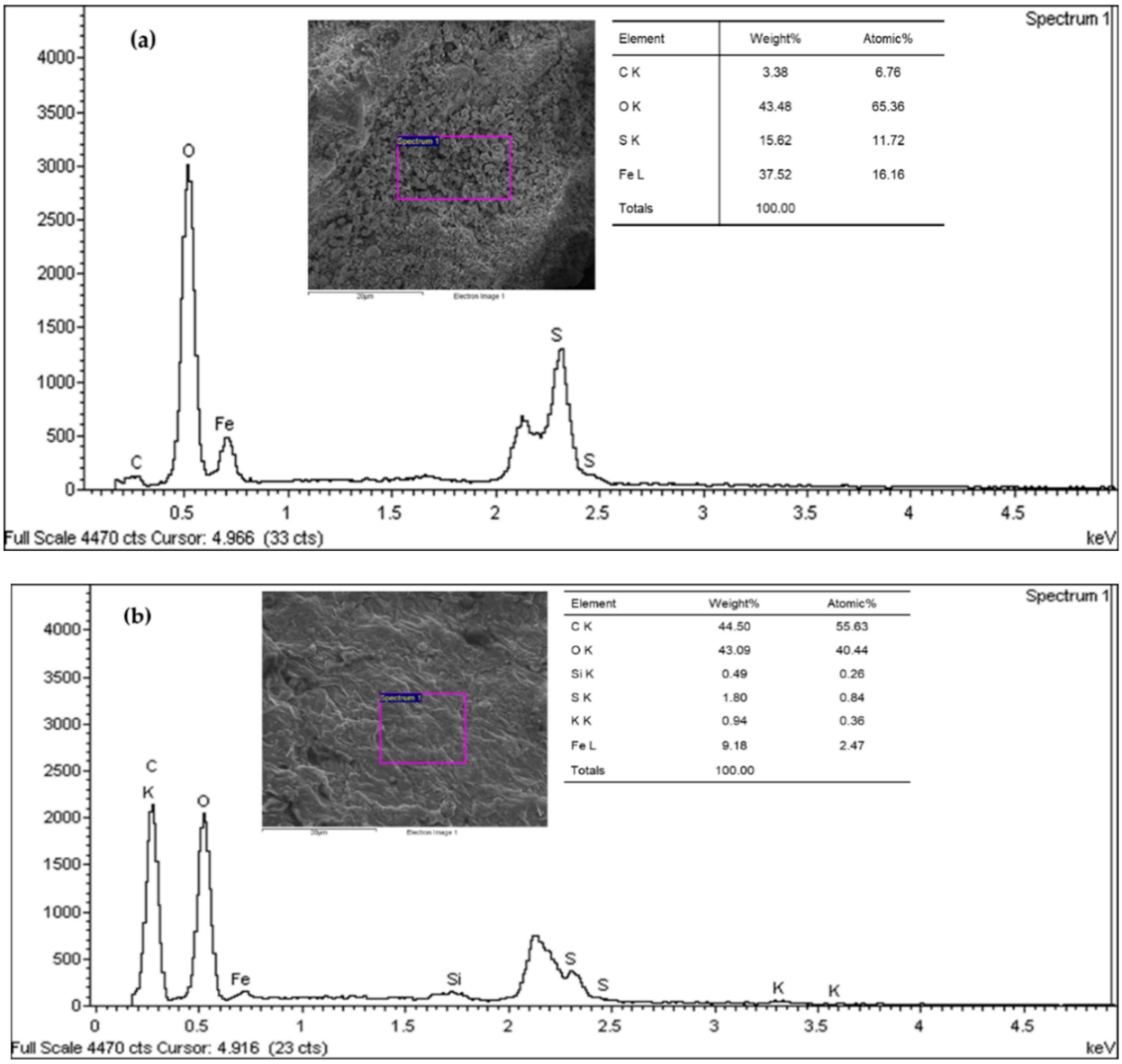

Figure 6. Energy-dispersive X-ray spectra of (**a**) raw $FeSO_4 \cdot H_2O$, and (**b**) sludge generated after coagulation.

Numerous advanced technologies have been implemented as a POME polishing technology for the elimination of colloidal and suspended particles from POME, including membrane filtration [16], Advance oxidation [37], electrocoagulation–peroxidation [14], and electrocoagulation [13]. The purpose of POME polishing technology is to minimize residual contaminants concentration and lower the prescribed industry effluent discharge limits set by the respective environmental agencies to conduct safe discharge of treated effluent [14,16]. Although these technologies were found effective in removing colloidal and suspended organic particles, all these technologies require high capital investment and operation costs. Therefore, these technologies are not suitable for implementation in large-scale POME treatment [14]. The remaining SS, COD, and BOD concentrations in treated POME were determined to be 28.27 ± 5 mg/L, 147 ± 3 mg/L, and 6.36 ± 0.5 mg/L, respectively, lower the stringent industry effluent discharge limits assigned by DOE, Malaysia.

Thus, the $FeSO_4 \cdot H_2O$ could be implemented as a potential coagulant for the post-treatment of POME to eliminate colloidal and suspended particles from POME. The implementation of $FeSO_4 \cdot H_2O$ as a coagulant in POME treatment would be beneficial for the palm oil industry in treating POME using an environmentally friendly coagulant

with lowing the treatment costs since $FeSO_4 \cdot H_2O$ is an industrial by-product. In addition, the presence of K, S, and Fe in the sludge reveals that the sludge generated after the coagulation–flocculation of POME could be utilized as a fertilizer for treating iron deficiency in plants [35].

4. Conclusions

In the present study, the post-treatment of POME was conducted using $FeSO_4 \cdot H_2O$ as a coagulant. The $FeSO_4 \cdot H_2O$ coagulation efficiency of POME was determined based on the elimination of SS, COD, and BOD with varying coagulant doses, pH, flocculation time, and flocculation speed. The second-order polynomial equation was well-fitted with experimental data. Additionally, pH, coagulant doses, and flocculation time significantly affected the elimination of SS, COD, and BOD from POME using $FeSO_4 \cdot H_2O$ as a coagulant. The maximum elimination of SS, COD, and BOD were about 97%, 98%, and 96%, respectively, were obtained at the optimized $FeSO_4 \cdot H_2O$ coagulation experimental condition of pH 4.7, $FeSO_4 \cdot H_2O$ doses of 1.82 g/L, flocculation time of 60 min and slow mixing speed of 30 rpm. The slow mixing speed had an insignificant effect on the COD and BOD removal, but it significantly affected SS elimination from POME. The pseudo-second-order kinetics equation was the best-described kinetics model, and the chemisorption would be the possible coagulation–adsorption mechanisms for the elimination of SS, COD, and BOD from POME using $FeSO_4 \cdot H_2O$ as a coagulant. The thermodynamics studies showed that the $FeSO_4 \cdot H_2O$ coagulation–flocculation of POME was endothermic and non-spontaneous. The residual SS, COD, and BOD concentrations in treated POME were 28.27 $\pm$ 5 mg/L, 147 $\pm$ 3 mg/L, and 6.36 $\pm$ 0.5 mg/L, respectively, lower than the assigned stringent industrial effluent discharge limits of DOE, Malaysia. Thus, the $FeSO_4 \cdot H_2O$ could be utilized as a potential coagulant for the post-treatment of POME to remove colloidal and suspended particles for safe discharge in a watercourse.

Author Contributions: Conceptualization, M.S.H. and A.N.A.Y.; methodology, S.A.R.; software, F.M.O.; validation, A.A.-G., M.Z. and Y.H.; formal analysis, A.N.A.Y.; investigation, M.Z.; resources, Y.H.; data curation, F.M.O.; writing—original draft preparation, M.S.H.; writing—review and editing, M.S.H.; visualization, S.A.R.; supervision, M.S.H.; project administration, A.N.A.Y.; funding acquisition, A.N.A.Y. All authors have read and agreed to the published version of the manuscript.

Funding: The APC was funded by the Centre for Research & Innovation, Universiti Kuala Lumpur (CoRI, UniKL), Kuala Lumpur, Malaysia.

Data Availability Statement: Not applicable.

Acknowledgments: The authors would like to thank the Ministry of Higher Education (MOHE), Malaysia, for financial support through the Fundamental Research Grant Scheme (FRGS/1/2019/TK10/USM/02/7).

Conflicts of Interest: The authors declare no conflict of interest.

References

1. Omar, A.K.M.; Norsalwani, T.L.T.; Asmah, M.S.; Badrulhisham, Z.Y.; Easa, A.M.; Omar, F.M.; Hossain, M.S.; Zuknik, M.H.; Norulaini, N.A.N. Implementation of the supercritical carbon dioxide technology in oil palm fresh fruits bunch sterilization: A review. *J. CO_2 Util.* **2018**, *25*, 205–215. [CrossRef]
2. Lee, M.D.; Lee, P.S. Performance of Chitosan and Polyglutamic Acid in Palm Oil Mill Effluent Treatment. In *Handbook of Research on Waste Diversion and Minimization Technologies for the Industrial Sector*; IGI Global: Hershey, PA, USA, 2021; pp. 147–173.
3. Wee, A.N.C.H.; Erison, A.E.; Anyek, E.H.E.; Pakpahan, G.R.; Lim, J.R.; Tiong, A.N.T. Techno-economic assessment of hydrogen production via steam reforming of palm oil mill effluent. *Sustain. Energy Technol. Assess.* **2022**, *53*, 102575. [CrossRef]
4. Ratnasari, A.; Syafiuddin, R.; Boopathy, S.; Malik, M.; Mehmood, R.A.; Amalia, D.; Prastyo, N.D.; Zaidi, S. Advances in pretreatment technology for handling the palm oil mill effluent: Challenges and prospects. *Bioresour. Technol.* **2022**, *344*, 126239. [CrossRef] [PubMed]
5. Loh, S.K.; Nasrin, A.B.; Azri, S.M.; Adela, B.N.; Muzzammil, N.; Jay, T.D.; Eleanor, R.A.S.; Lim, W.S.; Choo, Y.M.; Kaltschmitt, M. First Report on Malaysia's experiences and development in biogas capture and utilization from palm oil mill effluent under the Economic Transformation Programme: Current and future perspectives. *Renew. Sustain. Energy Rev.* **2017**, *74*, 1257–1274.

6. DoE. *Environmental Quality Act 1974, Environmental Quality (Industrial Effluent) Regulations 2009*; Department of Environment, Ministry of Science, Technology and the Environment: Kuala Lumpur, Malaysia, 2009.
7. Madaki, Y.S.; Seng, L. Pollution control: How feasible is zero discharge concepts in Malaysia palm oil mills. *Am. J. Eng. Res.* **2013**, *2*, 239–252.
8. Mohammad, S.; Baidurah, S.; Kobayashi, T.; Ismail, N.; Leh, C.P. Palm Oil Mill Effluent Treatment Processes—A Review. *Processes* **2021**, *9*, 739. [CrossRef]
9. Soo, P.L.; Bashir, M.J.K.; Wong, L.-P. Recent advancements in the treatment of palm oil mill effluent (POME) using anaerobic biofilm reactors: Challenges and future perspectives. *J. Environ. Manag.* **2022**, *320*, 115750. [CrossRef]
10. Ahmed, M.B.; Zhou, J.L.; Ngo, H.H.; Guo, W.; Thomaidis, N.S.; Xu, J. Progress in the biological and chemical treatment technologies for emerging contaminant eliminationfrom wastewater: A critical review. *J. Hazard. Mater.* **2017**, *323*, 274–298. [CrossRef]
11. Adeleke, O.A.; Latiff, A.A.A.; Saphira, M.R.; Daud, Z.; Ismail, N.; Ahsan, A.; Aziz, N.A.A.; Ndah, M.; Kumar, V.; Adel, A.-G.; et al. 2—Locally Derived Activated Carbon from Domestic, Agricultural and Industrial Wastes for the Treatment of Palm Oil Mill Effluent. In *Nanotechnology in Water and Wastewater Treatment*; Ahsan, A., Ismail, A.F., Eds.; Elsevier: Amsterdam, The Netherlands, 2019; pp. 35–62.
12. Charles, A.; Cheng, C.K. Photocatalytic treatment of palm oil mill effluent by visible light-active calcium ferrite: Effects of catalyst preparation technique. *J. Environ. Manag.* **2019**, *234*, 404–411. [CrossRef]
13. Mujeli, M.; Hussain, S.A.; Ismail, M.H.S.; Biak, D.R.A.; Jami, M.S. Screening of electrocoagulation process parameters for treated palm oil mill effluent using minimum-runs resolution IV design. *Int. J. Environ. Sci. Technol.* **2019**, *16*, 811–820. [CrossRef]
14. Bashir, M.J.K.; Lim, J.H.; Amr, S.S.A.; Wong, L.P.; Sim, Y.L. Post treatment of palm oil mill effluent using electro-coagulation-peroxidation (ECP) technique. *J. Clean. Prod.* **2019**, *208*, 716–727. [CrossRef]
15. Hossain, M.S.; Omar, F.; Asis, A.J.; Bachmann, R.T.; Sarker, M.Z.I.; Kadir, M.O.A. Effective treatment of palm oil mill effluent using $FeSO_4 \cdot H_2O$ waste from titanium oxide industry: Coagulation adsorption isotherm and kinetics studies. *J. Clean. Prod.* **2019**, *219*, 86–98. [CrossRef]
16. Ahmad, A.L.; Idris, I.; Chan, C.Y.; Ismail, S. Reclamation from palm oil mill effluent using an integrated zero discharge membrane-based process. *Pol. J. Chem. Technol.* **2015**, *17*, 49–55.
17. Gázquez, M.J.; Contreras, M.; Pérez-Moreno, S.M.; Guerrero, J.L.; Casas-Ruiz, M.; Bolívar, J.P. A Review of the Commercial Uses of Sulphate Minerals from the Titanium Dioxide Pigment Industry: The Case of Huelva (Spain). *Minerals* **2021**, *11*, 575. [CrossRef]
18. Poblete, R.; Otal, E.; Vilches, L.F.; Vale, J.; Fernández-Pereira, C. Photocatalytic degradation of humic acids and landfill leachate using a solid industrial by-product containing TiO_2 and Fe. *Appl. Catal. B Environ.* **2011**, *102*, 172–179. [CrossRef]
19. Erdem, E.; Donat, R.; Esen, K.; Tunç, T. Eliminationof soluble Cr (VI) in cements by ferrous sulphate monohydrate, solid lignin and other materials. *Ceram.-Silik.* **2011**, *55*, 85–93.
20. Rajniak, J.; Giehl, R.F.H.; Chang, E.; Murgia, I.; von Wirén, N.; Sattely, E.S. Biosynthesis of redox-active metabolites in response to iron deficiency in plants. *Nat. Chem. Biol.* **2018**, *14*, 442–450. [CrossRef]
21. Mensah-Akutteh, H.; Buamah, R.; Wiafe, S.; Nyarko, K.B. Optimizing coagulation–flocculation processes with aluminium coagulation using response surface methods. *Appl. Water Sci.* **2022**, *12*, 188. [CrossRef]
22. Ravikumar, K.; Krishnan, S.; Ramalingam, S.; Balu, K. Optimization of process variables by the application of response surface methodology for dye removal using a novel adsorbent. *Dye. Pigment.* **2007**, *72*, 66–74. [CrossRef]
23. Siyar, M.; Lashkarbolooki, M. Evaluation of the interfacial tension of binary surfactant mixtures and crude oil using the response surface method. *J. Mol. Liq.* **2022**, *366*, 120253.
24. Ilias, M.K.M.; Hossain, M.S.; Ngteni, R.; Al-Gheethi, A.; Ahmad, H.; Omar, F.M.; Naushad, M.; Pandey, S. Environmental Remediation Potential of Ferrous Sulfate Waste as an Eco-Friendly Coagulant for the Eliminationof NH_3-N and COD from the Rubber Processing Effluent. *Int. J. Environ. Res. Public Health* **2021**, *18*, 12427. [CrossRef] [PubMed]
25. Shadi, A.M.H.; Kamaruddin, M.A.; Niza, N.M.; Omar, F.M.; Hossain, M.S. Facile isotherms of iron oxide nanoparticles for the effectively removing organic and inorganic pollutants from landfill leachate: Isotherms, kinetics, and thermodynamics modelling. *J. Environ. Chem. Eng.* **2022**, *10*, 107753. [CrossRef]
26. Moghaddam, S.S.; Moghaddam, M.R.A.; Arami, M. Coagulation/flocculation process for dye eliminationusing sludge from water treatment plant: Optimization through response surface methodology. *J. Hazard. Mater.* **2010**, *175*, 651–657. [CrossRef]
27. Hossain, M.S.; Rahman, N.N.N.A.; Balakrishnan, V.; Alkarkhi, A.F.M.; Rajion, Z.A.; Kadir, M.O.A. Optimizing supercritical carbon dioxide in the inactivation of bacteria in clinical solid waste by using response surface methodology. *Waste Manag.* **2015**, *38*, 462–473. [PubMed]
28. Kozak, M.; Piepho, H.-P. What's normal anyway? Residual plots are more telling than significance tests when checking ANOVA assumptions. *J. Agron. Crop Sci.* **2018**, *204*, 86–98.
29. Ngteni, R.; Hossain, M.S.; Kadir, M.O.A.; Asis, A.J.; Tajudin, Z. Kinetics and Isotherm Modeling for the Treatment of Rubber Processing Effluent Using Iron (II) Sulphate Waste as a Coagulant. *Water* **2020**, *12*, 1747.
30. Muthusaravanan, S.; Sivarajasekar, N.; Vivek, J.S.; Paramasivan, T.; Naushad, M.; Prakashmaran, J.; Gayathri, V.; Al-Duaij, O.K. Phytoremediation of heavy metals: Mechanisms, methods and enhancements. *Environ. Chem. Lett.* **2018**, *16*, 1339–1359.
31. Shadi, M.H.; Kamaruddin, M.A.; Niza, N.M.; Emmanuel, M.I.; Hossain, M.S.; Ismail, N. Electroflotation treatment of stabilized landfill leachate using titanium-based electrode. *Int. J. Environ. Sci. Technol.* **2021**, *18*, 2425–2440.

32. Mohamad, N.A.; Hamzah, S.; Harun, M.H.C.; Ali, A.; Rasit, N.; Awang, M.; Rahman, W.R.W.A.; Azmi, A.A.A.R.; Habib, A.A.A.; Zahid, M.S.A.; et al. Integration of copperas and calcium hydroxide as a chemical coagulant and coagulant aid for efficient treatment of palm oil mill effluent. *Chemosphere* **2021**, *281*, 130873. [CrossRef]
33. Sharma, G.; Thakur, B.; Kumar, A.; Sharma, S.; Naushad, M.; Stadler, F.J. Atrazine eliminationusing chitin-cl-poly(acrylamide-co-itaconic acid) nanohydrogel: Isotherms and pH responsive nature. *Carbohydr. Polym.* **2020**, *241*, 116258. [CrossRef]
34. Nourani, M.; Baghdadi, M.; Javan, M.; Bidhendi, G.N. Production of a biodegradable flocculant from cotton and evaluation of its performance in coagulation-flocculation of kaolin clay suspension: Optimization through response surface methodology (RSM). *J. Environ. Chem. Eng.* **2016**, *4*, 1996–2003. [CrossRef]
35. Rodrigues, C.S.D.; Madeira, L.M.; Boaventura, R.A.R. Treatment of textile dye wastewaters using ferrous sulphate in a chemical coagulation/flocculation process. *Environ. Technol.* **2013**, *34*, 719–729. [PubMed]
36. Chung, C.Y.; Selvarajoo, A.; Sethu, V.; Koyande, A.K.; Arputhan, A.; Lim, Z.C. Treatment of palm oil mill effluent (POME) by coagulation flocculation process using peanut–okra and wheat germ-okra. *Clean Technol. Environ. Policy* **2018**, *20*, 1951–1970. [CrossRef]
37. Bello, M.M.; Raman, A.A.A. Trend and current practices of palm oil mill effluent polishing: Application of advanced oxidation processes and their future perspectives. *J. Environ. Manag.* **2017**, *198*, 170–182. [CrossRef] [PubMed]